STRESSES DEVELOPED IN QUARTER SPACE
Part 2 : Parametric Study

Hisham Hamdi Abdelmohsen
Structure Engineering Department, Faculty of Engineering,
Alexandria University, Alexandria, Egypt.

ABSTRACT

This is the second part of an article that deals with stresses in quarter space. Theoretical analysis is contained in part 1. The current presentation concerns with all stresses existing in quarter space geometry loaded in unsymmetric pattern. Effect of various parameters such as; apex angle, load position, and location coordinates on the induced stresses are investigated. Stress singularities are studied and assessed. Results evaluated here are fairly general and could be used via superposition for other normal traction shapes and intensity of loading.

Keywords: Quarter Space, Stresses, Infinite Wedge, Unsymmetric Loadings.

NUMERICAL ANALYSIS

The quarter space geometry and coordinate system are shown in Figure (1).

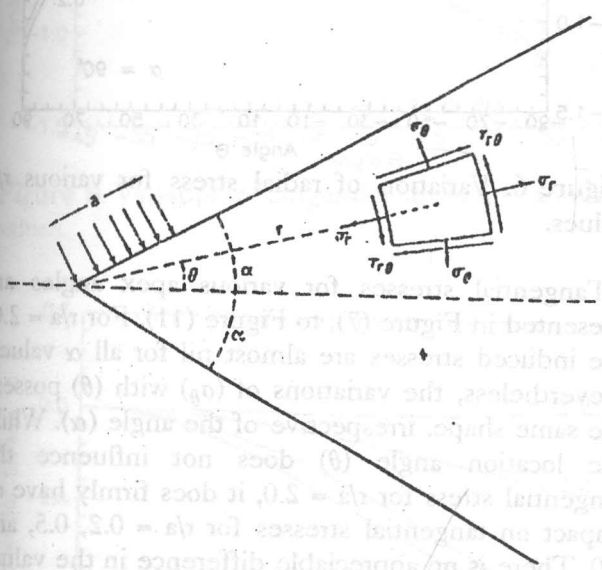

Figure 1. Geometry, coordinates, and loading.

Pursuing the analysis detailed in Part 1, Abdelmohsen (1997), the infinite integrals in (22), (23) and (24) are evaluated using Hermite polynomials $H_n(x)$, Abramowitz et al. (1970), i. e,

$$\int_{-\infty}^{\infty} f(x)\,dx \cong \Sigma_{i=1}^{n} w_i\, e^{x_i^2} f(x_i) + R_n \quad (1)$$

The abscissas x_i is the i^{th} zero of $H_n(x)$, and w_i is the weight given by $\dfrac{2^{n-1}\, n!\, \sqrt{\pi}}{n^2 [H_{n-1}(x_i)]^2}$.

R_n is the remainder defined by the equation

$$R_n = \frac{n!\sqrt{\pi}}{2^n\,(2n)!} f^{2n}(\xi) \quad (-\infty < \xi < \infty)$$

$f^{2n}(\xi)$ is the $2n^{th}$ derivative evaluated at point ξ. "n" is set equal to 20 in (1).

RESULTS

Figure (2) through Figure (6) illustrate the variation of radial stresses with location coordinates r, and θ. a is the length of the loaded segment. It is clear that the smaller is the apex angle, the higher is the rate at which the radial stress changes with the location angle θ. The radial stress does not seem to alter for r/a = 2.0, and r/a = 1.0. The linear variation shown in the radial stress value for small α has, in fact, changed in both rate, and even sign for higher α. Such results reflect the strong effect of the apex angle on radial stress alteration within the space.

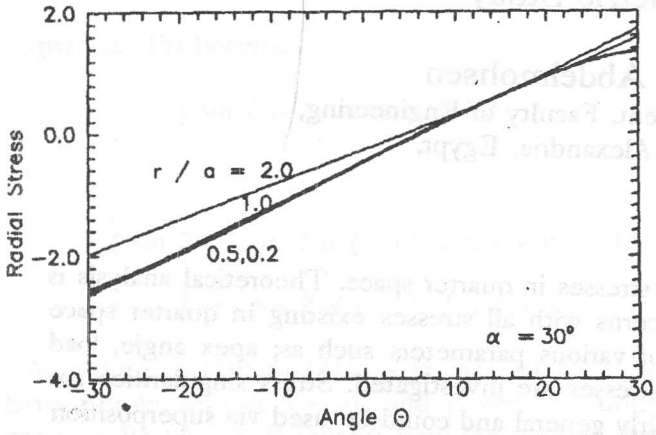

Figure 2. Variation of radial stress for various r/a values.

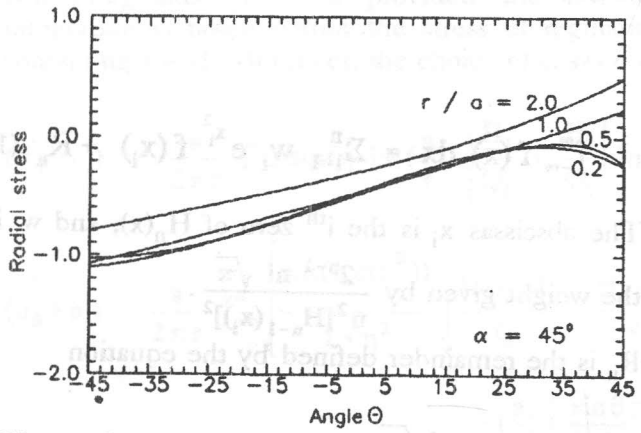

Figure 3. Variation of radial stress for various r/a values.

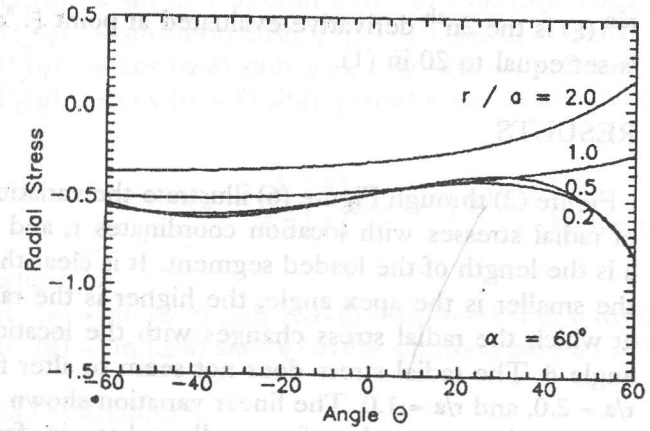

Figure 4. Variation of radial stress for various r/a values.

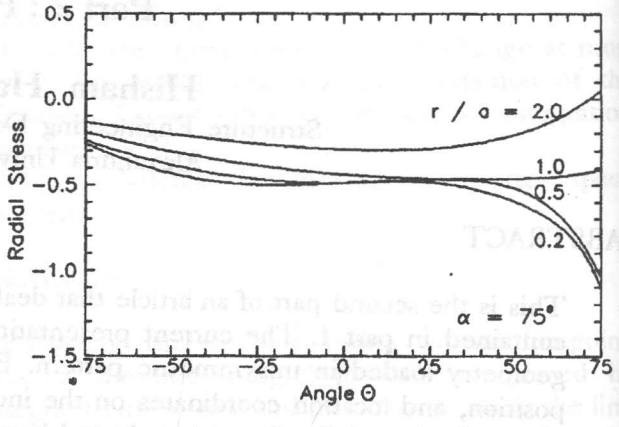

Figure 5. Variation of radial stress for various r/a values.

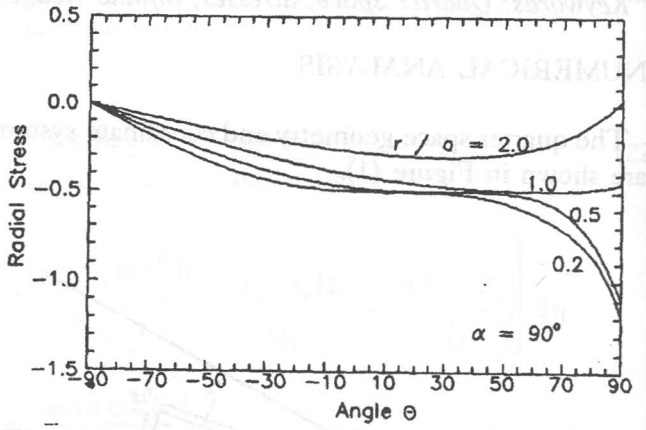

Figure 6. Variation of radial stress for various r/a values.

Tangential stresses for various apex angles are presented in Figure (7), to Figure (11). For r/a = 2.0, the induced stresses are almost nil for all α values. Nevertheless, the variations of (σ_θ) with (θ) possess the same shape, irrespective of the angle (α). While the location angle (θ) does not influence the tangential stress for r/a = 2.0, it does firmly have an impact on tangential stresses for r/a = 0.2, 0.5, and 1.0. There is no appreciable difference in the values correspond to r/a = 0.50, and r/a = 0.20, with respect to either the shape or the value, especially for lower values of (α).

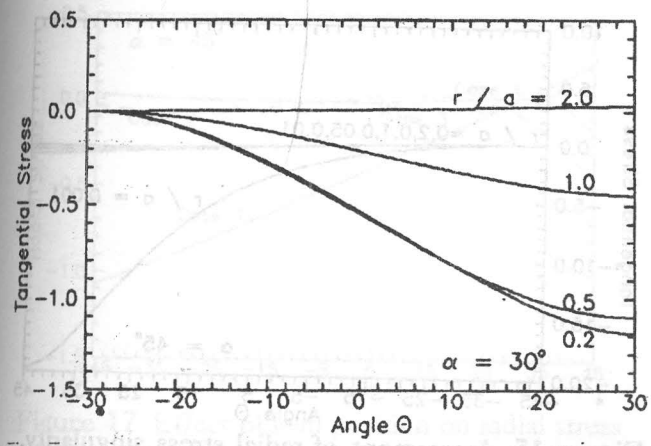

Figure 7. Variation of tangential stress for various r/a values.

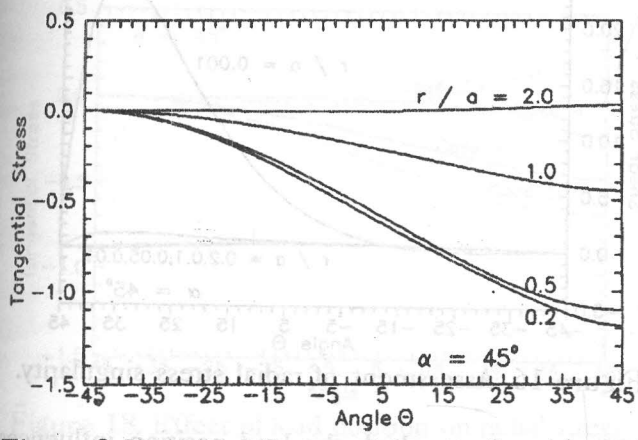

Figure 8. Variation of tangential stress for various r/a values.

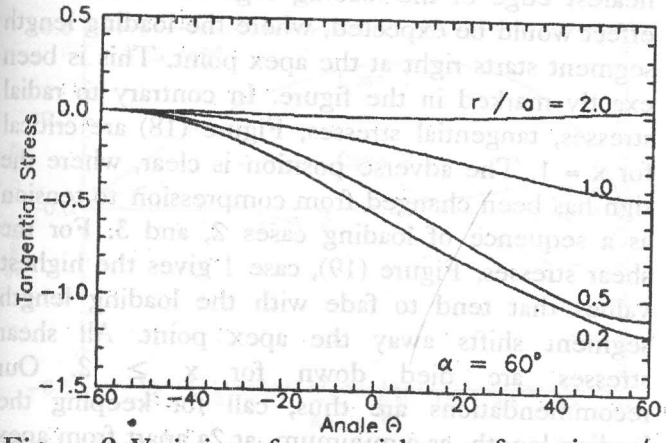

Figure 9. Variation of tangential stress for various r/a values.

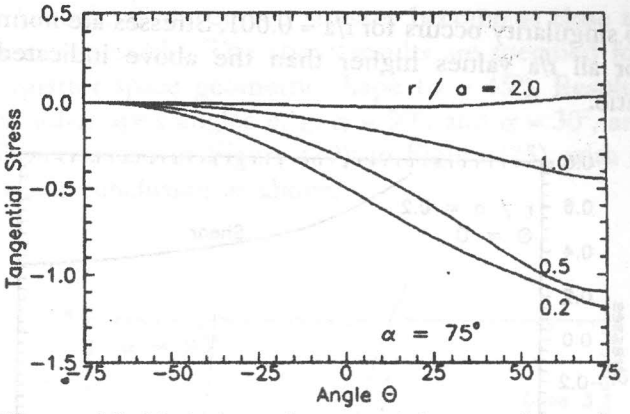

Figure 10. Variation of tangential stress for various r/a values.

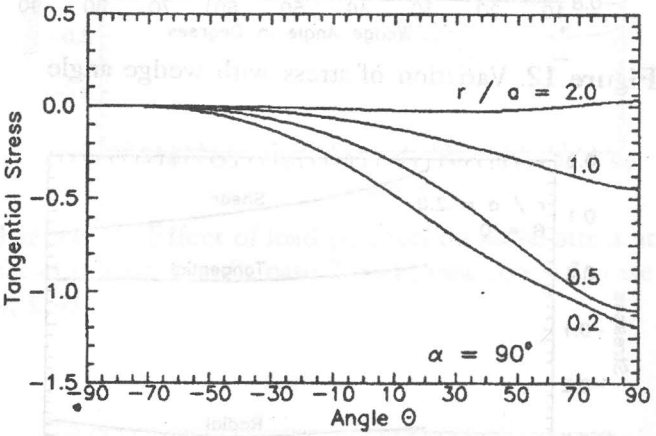

Figure 11. Variation of tangential stress for various r/a values.

To further assess the effect of angle (α) on all stresses at points fall on the symmetry line ($\theta = 0$), Figures (12), and (13) are created. Comparison is selected at space symmetry line to offset the boundary effects on the solution. Both radial and tangential stresses at symmetry line are close to behave independently on the angle (α). On the other hand, the shear stresses behave differently, as such, they tend to be smaller in value with the increase in (α). The above results stand for a wide range of r/a values, e. g. r/a = 0.20, and up to r/a = 2.0.

It was necessary to substantiate the singular nature of the existing boundary value problem, due to the appearance of the term (a/r) in the final stress formulation Eqs. (22), (23), and (24) Ref. (11). Figure (14) through (16) illustrate the assessment of stress singularity. For $\alpha = 45°$, the adverse effect due

to singularity occurs for r/a = 0.001. Stresses are norm for all r/a values higher than the above indicated ratio.

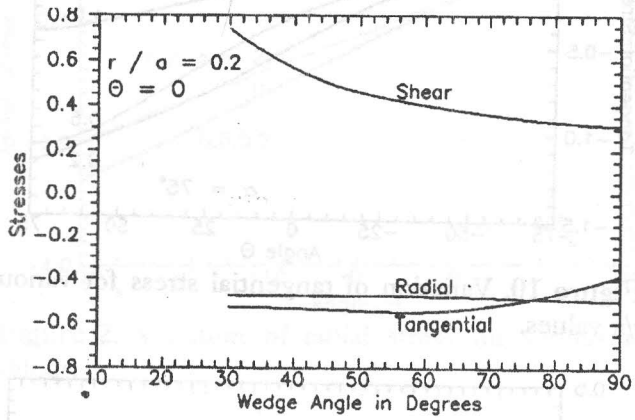

Figure 12. Variation of stress with wedge angle

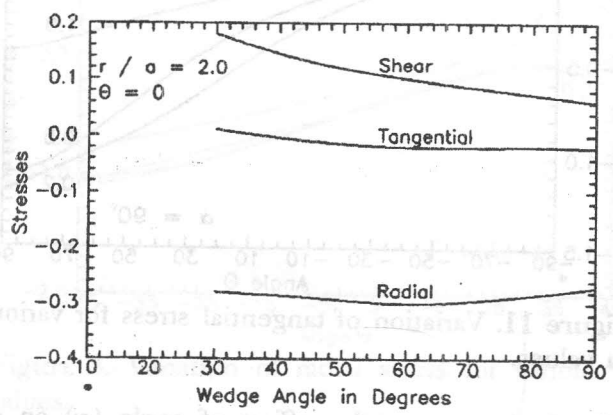

Figure 13. Variation of stress with wedge angle

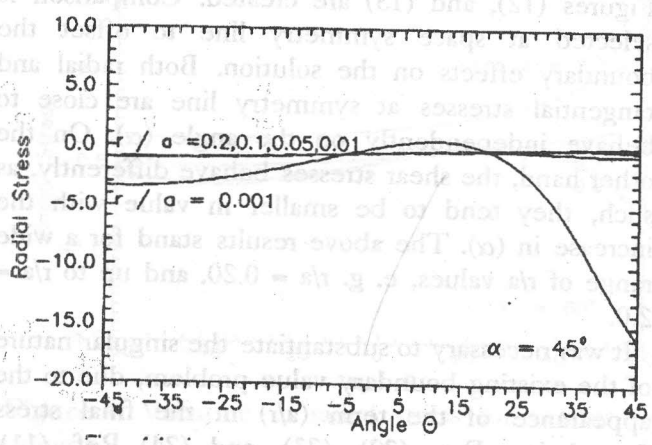

Figure 14. Assessment of radial stress singularity.

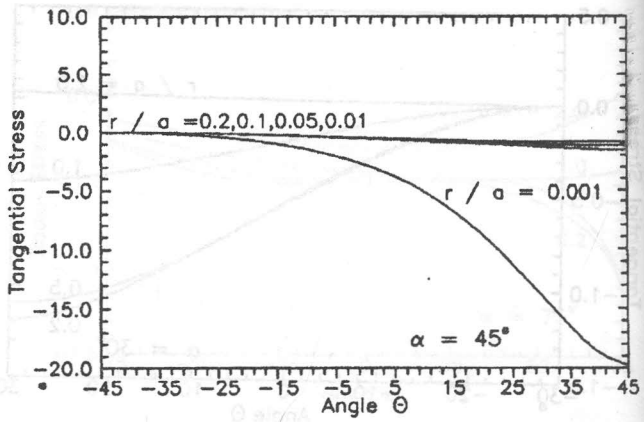

Figure 15. Assessment of radial stress singularity.

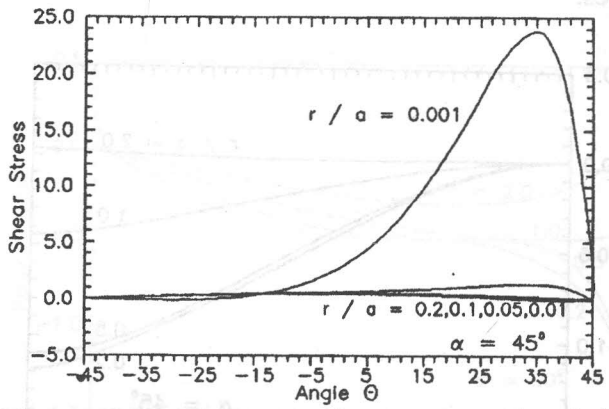

Figure 16. Assessment of radial stress singularity.

The degree at which the load position influences radial stresses is given in Figure (17). "x" is the ratio relates the distance between the apex point and the nearest edge of the loading segment. The utmost effect would be expected, where the loading length segment starts right at the apex point. This is been exactly marked in the figure. In contrary to radial stresses, tangential stresses, Figure (18) are critical for x = 1. The adverse position is clear, where the sign has been changed from compression to tension as a sequence of loading cases 2, and 3. For the shear stresses, Figure (19), case 1 gives the highest values that tend to fade with the loading length segment shifts away the apex point. All shear stresses are died down for $x \geq 2$. Our recommendations are thus, call for keeping the loading length, as a minimum, at 2a apart from apex point.

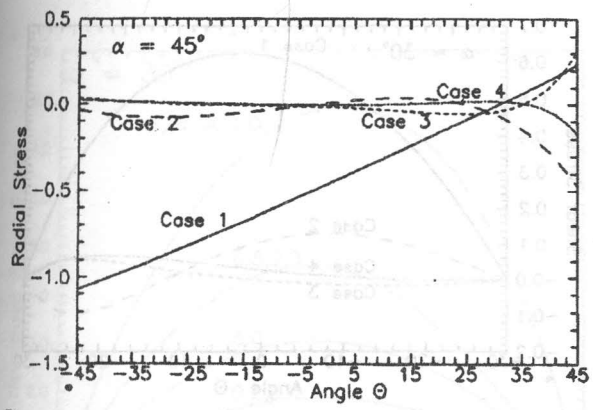

Figure 17. Effect of load position on radial stress at r/a =1.0 (case 1; x=0., case 2; x=1., case 3; x = 2., case 4; x =3).

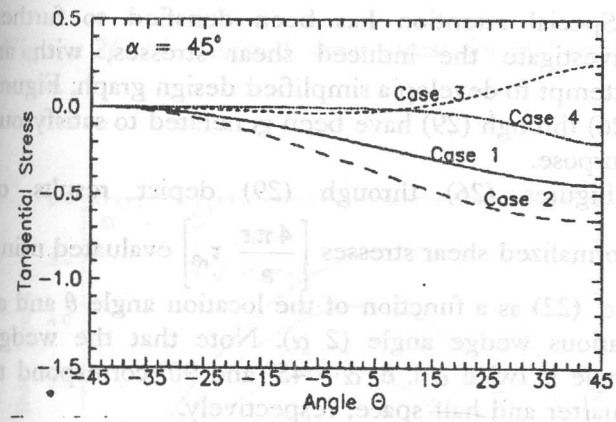

Figure 18. Effect of load position on radial stress at r/a =1.0 (case 1; x=0., case 2; x=1., case 3; x = 2., case 4; x =3).

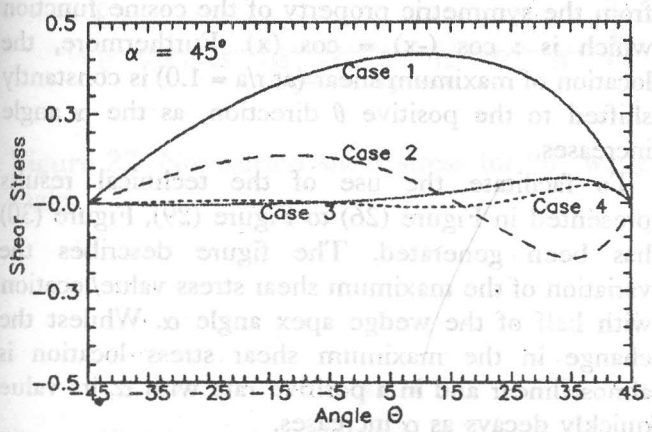

Figure 19. Effect of load position on radial stress at r/a =1.0 (case 1; x=0., case 2; x=1., case 3; x = 2., case 4; x =3).

As such, all developed stresses become as close to zero as possible. The above results are specified for a quarter space geometric shape (α = 45°). Results for other apex angles e. g. α = 90°, and α = 30°, are demonstrated in Figure (20), to Figure (25), with a similar conclusion as above.

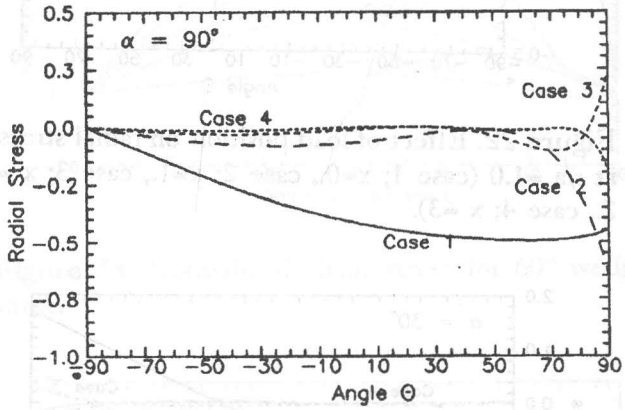

Figure 20. Effect of load position on radial stress at r/a =1.0 (case 1; x=0., case 2; x=1., case 3; x = 2., case 4; x =3).

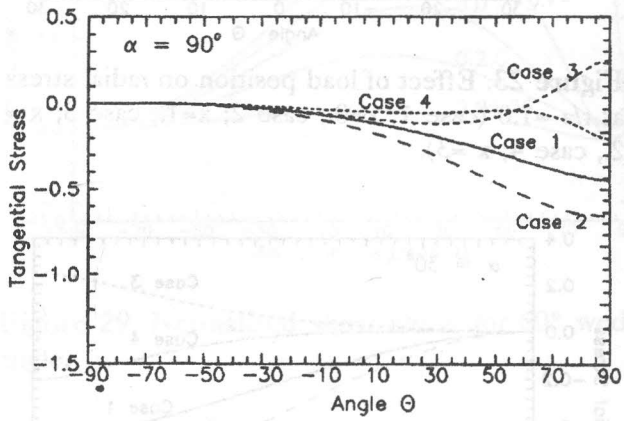

Figure 21. Effect of load position on radial stress at r/a =1.0 (case 1; x=0., case 2; x=1., case 3; x = 2., case 4; x =3).

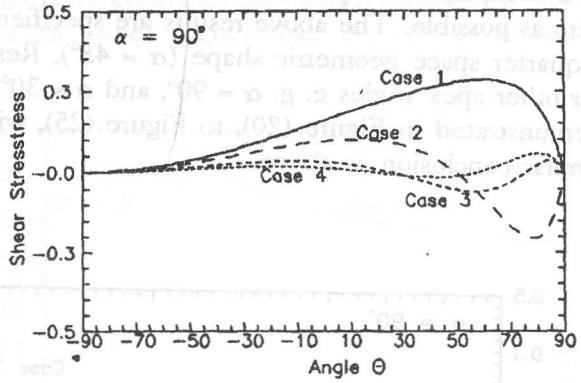

Figure 22. Effect of load position on radial stress at r/a =1.0 (case 1; x=0., case 2; x=1., case 3; x = 2., case 4; x =3).

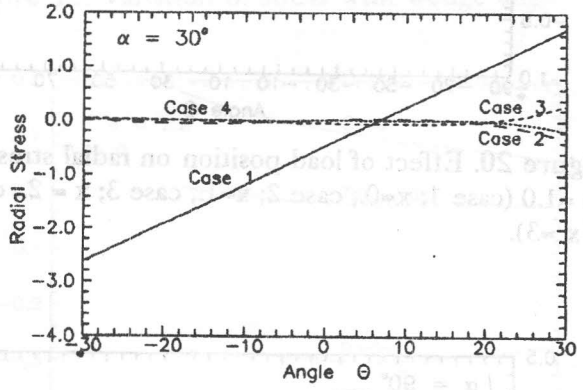

Figure 23. Effect of load position on radial stress at r/a =1.0 (case 1; x=0., case 2; x=1., case 3; x = 2., case 4; x =3).

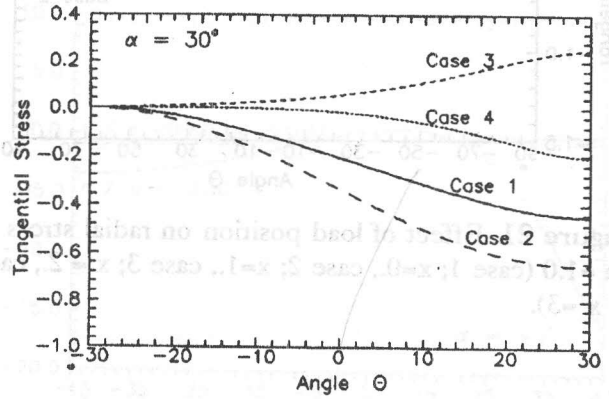

Figure 24. Effect of load position on radial stress at r/a =1.0 (case 1; x=0., case 2; x=1., case 3; x = 2., case 4; x =3).

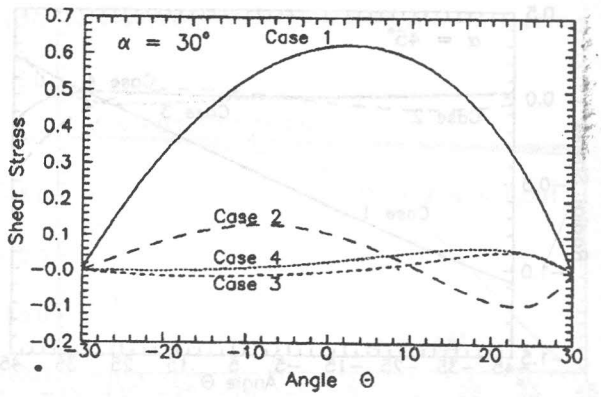

Figure 25. Effect of load position on radial stress at r/a =1.0 (case 1; x=0., case 2; x=1., case 3; x = 2., case 4; x =3).

Special attention has been densfied to further investigate the induced shear stresses, with an attempt to develop a simplified design graph. Figure (26) through (29) have been generated to satisfy our purpose.

Figures (26) through (29) depict results of normalized shear stresses $\left[\frac{4\pi r}{a}\ \tau_{r\theta}\right]$ evaluated using Eq. (22) as a function of the location angle θ and at various wedge angle (2 α). Note that the wedge angle is twice α i. e. α = 45° and 90° correspond to quarter and half space, respectively.

It is clear from (22) that $\tau_{r\theta}$ depends on the value of cos (η In (a/r)), which yields the same $\tau_{r\theta}$ value for certain a/r ratio and its inverse r/a, i. e., r/a = 0.50, and a/r = 2.0, r/a = 0.20 and a/r = 5.0. This extends from the symmetric property of the cosine function which is : cos (-x) = cos (x). Furthermore, the location of maximum shear (at r/a = 1.0) is constantly shifted to the positive θ direction, as the α angle increases.

To facilitate the use of the technical results presented in Figure (26) to Figure (29), Figure (30) has been generated. The figure describes the variation of the maximum shear stress value/location with half of the wedge apex angle α. Whilest the change in the maximum shear stress location is almost linear and in a positive rate with α, its value quickly decays as α increases.

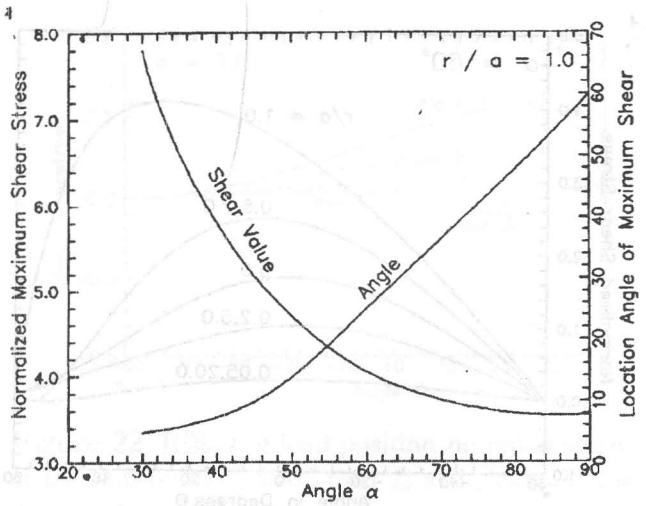

Figure 30. Value and location of Normalized maximum shear stress.

CONCLUSION

The results presented in the article are fairly comprehensive. They demonstrate all developed stresses in a quarter space loaded in unsymmetric pattern. Effect of apex angle, and load position are assessed. Developed equations are easy to be fed into a short computer program so as to generate answers for actual apex angle, and for a general boundary loading conditions. The 30 figures illustrated here, have been intended to cover a wide range of design variables that might exist in practical engineering cases.

REFERENCES

[1] M. Abramowitz, and I. A. Stegun. *Handbook of Mathematical Functions*, Dover Publications, Inc., New York, 1970, pp. 890 .

l[2] S.D. Carothers, "Plane Strain in a Wedge", *Proceedings, Royal Society*, Edinburgh, Vol. 23, 1912, pp. 292.

[3] R.D. Cook, *Concepts and Application of Finite Element Analysis*, 2nd edition, John Wiley & Sons, Inc. New York, 1981.

[4] O.V. Estrorff and E. Kousel, "Coupling of Boundary and Finite Elements for Soil - Structure Interaction Problems, *"Earthquake Eng. and Structural Dynamics*, Vol. 18, 1989, pp. 1065 - 1075.

[5] M. Hetenyi, "A Method of Solution for the Elastic Quarter - Plane", *J. of Applied Mechanics*, June 1960, pp 189.

[6] F.B. Hildbrand, *Advanced Calculus for Application*, 2nd edition, Prentice - Hall Inc. , 1976.

[7] C.E. Inglis, "Some Special Cases of Two - Dimensional Stress and Strain, *"Transactions of Institution of Xlavnl Archetete*, Vol. 64, 1922, pp. 253.

[8] S. Timoshenko and J. H. Goodier, *Theory of Elasticity*, Second Edition, McGraw-Hill Book Company, Inc. New York, N. T. , 1951.

[9] C.I. Tranter, "The Use of the Mellin Transform in Finding The Stress Distribution on an Infinite Wedge", *The Quarterly Journal of Mechanics and Applied Mathematics*, Vol. 1, 1948, pp. 125 - 130.

[10] M.L. Willams, "Stress Singularities Resulting From Various Boundary Conditions in Angular Corners of Plates in Extension", *J. of Applied Mechanics*, Dec., 1952, pp. 526.

[11] H.H. Abdelmohsen, "Stresses Developed in Quarter Space; Part 1 : Theory", Alexandria Engineering Journal, June 1997.